THE STRUCTURE AND BRIEF REVIEW ON $Ba(NO_3)_2$, KNO_3 AND DISPERSED SOLID ELECTROLYTES

I STRUCTURE OF $Ba(NO_3)_2$ AND KNO_3

I.1 $Ba(NO_3)_2$

Barium nitrate is an isomorphous crystal with other nitrates such as Ca, Sr & Pb forming a group. It has a cubic structure with the space group Pa_3 and it belong to T_h^6 class [1]. In the cubic system the symbol 'T' is used for tetrahedral symmetry group with four triad and three diad axes.

CaF_2 in its naturally occurring form is called the 'fluorite' and the compounds which crystallize in this form are called fluorites. The Nitrates of Ca, Ba, Sr and Pb are isomorphous and have fluorite type structure [1]. The two- and three-dimensional structure of fluorite RX_2 lattice is shown in figure I.1. In a compound RX_2, each ion of species R is surrounded by eight equivalent nearest neighbor ions of species X forming the corners of a cube of which R is the center. Each ion of species X is surrounded by tetrahedron of four equivalent R ions. More fundamentally the structure has a face centered cubic translational group and a space lattice of symmetry O_h^5.

The structure is interpreted in terms of a primitive cube of side 'a'. It comprises three interpenetrating face centered cubic lattices. The first is a lattice of species R with its origin at the point (0,0,0) and with primitive translational vectors of (0, 1/2, 1/2) ; (1/2, 0, 1/2); and (1/2, 1/2, 0) in the cube of side a. The X species are located on two further lattices with similar translational vectors but with origins at (1/4, 1/4, 1/4) and at (3/4, 3/4, 3/4a). The site of the R ion has O_h symmetry, being at the centre of a cube of eight X ions.

It is apparent that the fluorite structure provides close contact between the different species of atom or ion. Furthermore, if the ions of species R are sufficiently large, close contact between the ions of species X is prevented. If the constituent species are regarded as hard spheres with radii of r(R) and r(X), contact occurs between the R and X ions to the exclusion of X-X contact and of R-R contact [2] when the radii satisfy the condition $4.45 \geq r(R) / r(X) \geq 0.73$.

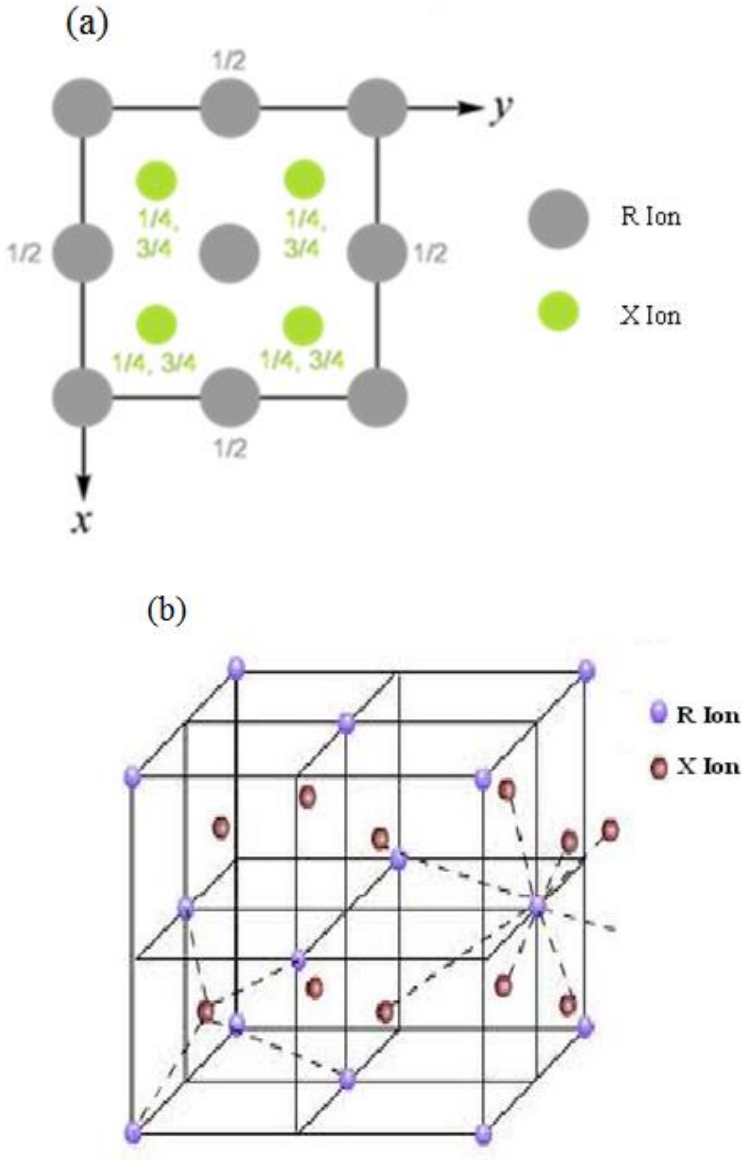

Fig.1.1 The Fluorite structure of the (a) two dimensional and (b) three dimensional RX_2 Lattice.

The possibility of close contact between dissimilar ions suggests that the fluorite structure will be favored by strongly ionic compounds with formula RX_2 which possess large ions of type R. In fact the R ions are normally relatively small and it is possible to find several series of compounds in which one is able to pass through the other limiting value, enabling contact between X ions to occur. For example, among the halides of cadmium or of barium one finds that the fluorite lattice structure occurs for the smaller halide (X) ions while the iodides possess orthorhombic or sheet like structures.

The materials found to possess the fluorite structure have been divided by Wyckoff [2] into four main classes:

i. The halides of the larger divalent cations (all but two are in fact fluorides) e.g., CaF_2, SrF_2, BaF_2, CdF_2, PbF_2, $SrCl_2$, $BaCl_2$.

ii. The oxides of certain large quadrivalent cations.

e.g., ZrO_2, CeO_2, ThO_2, and UO_2.

iii The oxides and other chalcogenides of alkali and other univalent cations.

e.g., K_2S, Na_2S and Li_2Se.

iv Miscellaneous intermetallic compounds and the oxy fluorides and hydrides of rare earth elements.

The nitrates of Ca, Sr, Ba and Pb are structurally similar to the compounds of the category (i) of the above classification. In $Ba(NO_3)_2$ the anion consisting of nitrogen at the centre and the oxygens occupying the corners of an equilateral triangle replaces the F^- ion of CaF_2 structure. There is a difference of opinion whether or not all the four atoms are coplanar. Two hypotheses have been proposed. The older opinion proposed by Vegard [3] where T_h^6 space group is assigned to them has four molecules in the unit cell. In this case all the NO_3 groups are similar and so there is an inversion center and all the three anions are coplanar with the nitrogen at the center.

In the second hypothesis proposed by Birnstock [4] based on neutron scattering measurements, T^4 space group is assigned. In this case two kinds of nitrate groups are distinguished and there is no center of inversion. The oxygens in this proposal are no more coplanar with the nitrogen, but are thought to be pyramidal with the nitrogen atom displaced from the plane of the oxygens. Bon et al [5] have carried out the studies of infrared reflection spectra on the single crystals of these isomorphous compounds. The results were discussed and they concluded that the T^4 structure is more appropriate on the basis of their studies.

Considering several properties of these crystals like the melting points, the solubility, thermal expansion, elastic constants, intensity of the Raman lines and the magneto-optic anomaly, srinivasan [6] has concluded that the bond between the metal ion and the nitrate ion is essentially ionic. The binding force of ionic crystals is due to coulomb attraction and is very high, giving rise to a high melting point. Since there are no free electrons ideally, we expect poor electrical and thermal conductivity. At temperatures approaching the melting point the ions become mobile enough to result in some ionic conductivity. The lack of free electrons also implies good optical transparency over large portions of the electro-magnetic spectrum. Optical absorption does not occur until the photon energy is high enough to excite an electron out of one of the filled ionic shells at about 6eV, which corresponds to the far ultraviolet.

I.2 KNO_3

Potassium nitrate was discovered in 1958 as a ferroelectric material by Sawada et al [7]. Since then KNO_3 has been investigated by many researchers from the ferroelectric, dielectric, and structural view point [8]. It has been known since the late 1960s that KNO_3 exists in one of the several crystallographic phases depending on external state variables. Only one phase is ferroelectric (phase III) which is known to exist at elevated temperature while cooling from higher temperature.

This ferroelectric phase III would be of technological interest if it can be stabilized at room temperature. KNO_3 has been found to possess aragonite structure known as phase II by many researchers at room temperature.

The molecular structure of KNO_3 has been investigated for the first time by electron diffraction by patrov et al [9]. The first stage of structural analysis was performed on the assumption of a bidentate configuration of KNO_3 molecule with C_{2v} symmetry and with D_{3h} local symmetry of the NO_3 fragment. KNO_3 has been found to exist in variety of phases as shown in Table-I. On heating, the crystal structure changes from orthorhombic (phase-II) to rhombohedral (phase-I) and on cooling, the phase-I changes first to phase-III at about 124ºC which is ferroelectric and then to phase-III to phase-II at about 110ºC [10-13].

TABLE-I The different phases of KNO_3

Phase of KNO_3	**Temperature (ºC)**	**Unit –cell data (Å)**			**Crystal structure**
		a	B	C	
Phase II	130	5.414	9.164	6.431	Orthorhombic
Phase I	124	5.423	5.423	9.638	Rhombohedral
Phase III	110	5.430	5.430	9.095	Rhombohedral

The crystal structure and related parameters of different phases of KNO_3 are shown in figure I.2. The phase transitions also accompany the change in volume of the unit cell. The relative volume changes of KNO_3 unit cell associated with the phase II → phase I, phase I → phase III, phase III → phase II transitions are +0.27, -5.375, and -3.56 %, respectively [14].

The phase II → phase I transition increases the overall density of the loosely packed structure. However, the decrease in the volume during the phase I → phase III transition allows the structure to increase the packing density. This packing places the KNO_3 under an effective stress, which is known to affect the phase transition temperatures. This effective applied stress enhances the sintering of the KNO_3 particles [15].

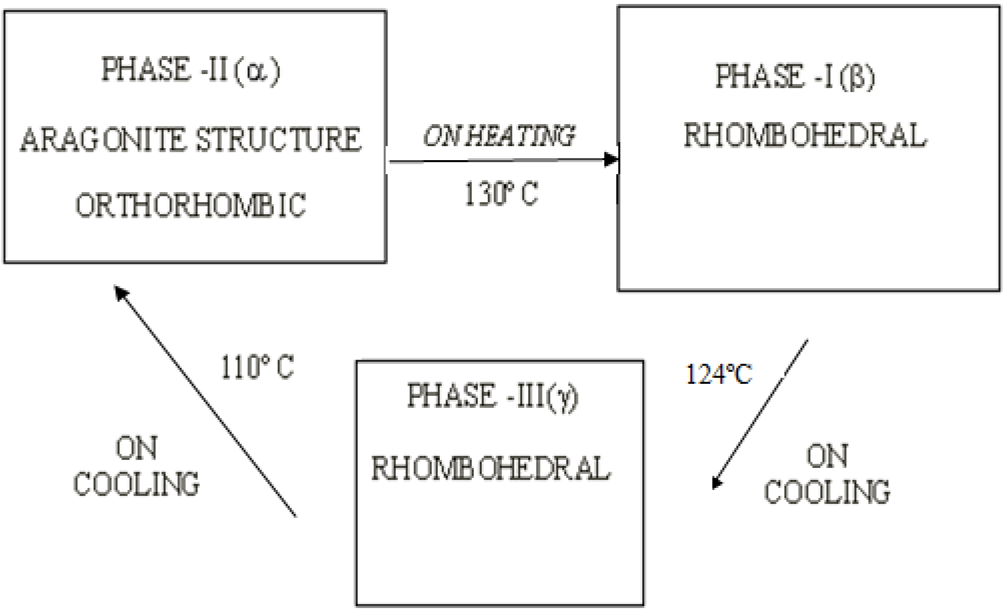

Fig.1.2 Crystal structure changes when KNO_3 was passed through the heating and cooling cycles.

The crystal structures of the phase I and phase II are non-polar, but that of the phase III is polar. The corresponding crystal structures of aragonite and γ-phase of KNO_3 can be seen in figures I.3(a) and 3.3(b) respectively. Aragonite is the stable phase of KNO_3 at room temperature and γ-phase is the rhombohedral unit cell in the ferroelectric phase III which contains one molecule of KNO_3 and K^+ ions occupy its corners whereas NO_3^- ion lies near its body center. The NO_3 group forms a regular triangle with the N atom at its center. The plane of the NO_3 group is perpendicular to the c-axis and it does not exist exactly at the body center [15]. Potassium nitrate is one of the several substances recommended [16] as a standard reference material in thermal analysis. The alkali nitrate crystals are dielectric ones with the variation in both the conductivity and the crystal structures at their phase transitions.

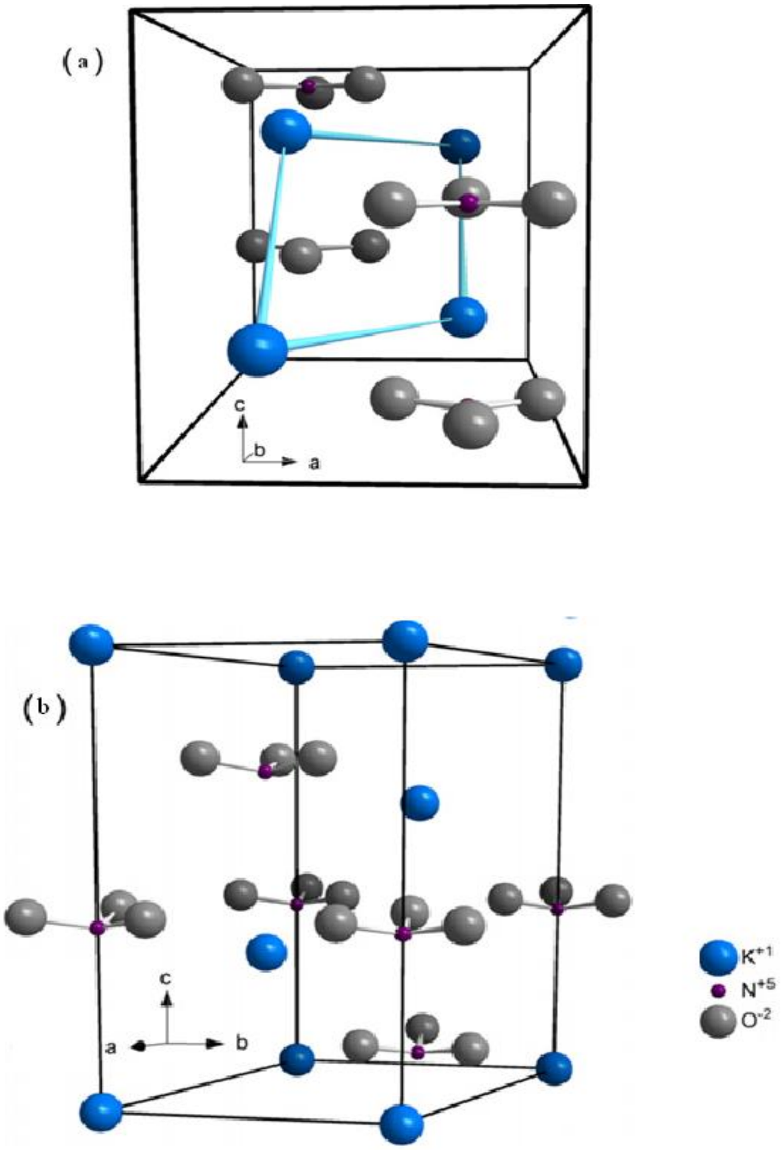

Fig 1.3 Crystal structure views of KNO_3 a) aragonite, (b) γ -phase.

II A BRIEF REVIEW ON DISPERSED SOLID ELECTROLYTES

Mixed crystals aroused considerable interest, curiosity and motivated extensive investigations because of their wide applications. During the last several years, considerable attention has been devoted to the study of transport processes in ionic crystals. Among the transport processes, conductivity studies provide valuable information on the state of point defects in ionic crystals. The ionic conductivity of such crystals at temperatures not very close to the melting point is due to the migration of positive ion vacancies [17].

Ionic conductivity measurements as a function of temperature have been done by a number of researchers. The most of the work is done on alkali halide crystals doped with anion as well as cation impurities [18-20], since they are easily obtainable ionic compounds of relatively simple crystal structure. However the work on mixed crystals is very limited. Lehfeldt[21], and Phipps and Patridge [22] investigated conductivities of several alkali halides, including KBr and KCl, while Kelting and Witt [23] established the effect of divalent impurities on conductivity. Ionic conductivity studies of Ambrose and Walace [24] on KCl-KBr mixed crystals showed that the conductivity of the mixed crystals is never far outside the range of conductivity fixed by the pure end components, indicating that the population of vacancies in mixed crystals is same as those in the pure end crystals. But the conductivity studies of Schultze[25], Annenkov et al [26], Arends et al [27], and Zayadowskaya et al[28] indicated that the concentration of vacancies in mixed crystals exceed that in the pure end components.

Ionic conductivity studies in KCl-KI mixed crystals have been done by U.V. Subbarao and V. Haribabu [29]. Ionic conductivity studies in KCl–NaCl mixed crystals were done by P.Veerasham et al [30]. Anomalous ionic conduction AgBr-AgI mixed crystals and multiphase systems have been studied by K.Shahi et al [31]. Growth and study of mixed crystals of Ca-Cd iodate were studied by S.L Garud et al [32]. Growth and characterization of mixed crystals of NaBr-KBr were studied by C.M. Padma et al[33]. The conclusion of these studies indicates that structure of defects for mixed crystals is different in contrast with their pure position. The difference of atomic size between mixed crystals cause to local stresses in lattice and this defect change crystal properties, and its lattice parameters [34]. In addition, mixed alkali halides found their applications in optical, opto-electronic and electronic devices.

The work on alkali and alkaline earth nitrates is very limited. Electronic structure of fluorite type compounds and mixed crystals was done by J. Kudrnovsky et al [35]. X-Ray diffractometry studies and lattice parameter calculation on KNO_3-NH_4NO_3 solid solution were studied by Wen-Ming Chien et al [36]. More recently, new attention has been paid to the fluorite-type compounds and derived mixed crystals in connection with their superionic conductivity. Survey of literature indicates that there is no work on dc ionic conductivity of mixed crystals comprising of alkaline earth nitrates as against alkali nitrates in general and no such conductivity work on $Ba(NO_3)_2$ and KNO_3 mixed crystals in particular.

The development of dispersed solid electrolytes can be linked to the observations made during the beginning of this century [37] that the conductivity of two phase mixtures may exceed the conductivities of pure constituents. Wagner [38] and Crosbie [39] studied the conductivity behavior of semiconductors, with small inclusions of another non-conducting phase and found that the conductivities exceeded those of pure constituents. Recently, this approach has been extended to solid electrolytes in order to bring about enhancements in their ionic conductivities. Most of the work reported in the literature has been done with the dispersion of insulators such as Al_2O_3, SiO_2, fly ash, ZrO_2 etc., in ionic conductors. Among these in the present work the alumina with particle size(1 µm, 0.3µm, 0.06µm), SiO_2(20nm), CeO_2(15nm) were used in the preparation of the dispersed solid electrolyte systems.

In the following sections review of the work already done in the form of dispersed solid electrolyte systems is presented exhaustively.

II.1 LITHIUM HALIDES

Liang [40] is almost the founder of studies on dispersed systems who first reported his results in Anhydrous LiI dispersed with Al_2O_3. As per his observations there was a maximum in conductivity of about 10^{-5} S/Cm at 25^0C at around 40 mole percent of Al_2O_3. It was found that the electronic conductivity of these systems was insignificant compared to the ionic conductivity. The conduction mechanism was attributed to the cation vacancies which are the species responsible for conduction in pure LiI. It was also confirmed by X-Ray diffractograms(XRD) that there was no indication of formation of any solid solution. The discharge and storage characteristics indicated that the system functioned as a practical, low rate solid-state battery system [41]. However, the conductivity studies [42] on $LiI.H_2O$ showed a significantly higher value than anhydrous LiI. The dispersion of Al_2O_3 or SiO_2 enhanced the conductivity further in this system. It was also suggested that the highest conductivity is reached with very fine alumina powder but alumina powders less than some critical radius are less effective.

$LiI\text{-}Al_2O_3$ composite system was investigated using NMR study which showed evidence for occurrence of highly conductive phase. The self diffusion constant of Li in this system was found to be 8.1×10^{-10} cm^2/sec at 300^oK which is 1600 times larger than that in pure LiI matrix. This is a reasonable order of magnitude to explain the enhanced conductivity quantitatively [43]. The effective surface properties of alumina upon the enhancement of conductivity in $LiI\text{-}Al_2O_3$ composite were studied [44] by measuring the thickness of the interface layer. Heat treatment of alumina resulted in a slight decrease of thickness of interfacial layer. The surface properties changed with this treatment. The extent of basic active sites, especially –OH group was found to have an effect on the conductivity enhancement. In their subsequent study [45] they realized further enhancement of conductivity when dispersed with particles of γ- Al_2O_3 whose surface was modified by adsorption of nitrates of alkali and alkaline earths and subsequent thermal decomposition at 800^0C.

Significant enhancement of conductivity was also noticed in other lithium halide dispersed systems that include: LiCl-Al_2O_3 [46], LiBr-H_2O-Al_2O_3(α, β) [47-49] with different dispersoids such as α- Al_2O_3, SiO_2, γ- Al_2O_3, η- Al_2O_3 in LiCl. In the case of η- Al_2O_3(25 m/o) the enhancement was about 2 orders of magnitude measured at 25^0C and the activation energy was found to decrease by half of that for LiCl. Nakamura and Goodenough [47] reported a maximum enhancement of about 2 orders at 43^0C for LiBr.H_2O-Al_2O_3(40 m/o), a maximum of 2 orders of magnitude was also measured by Slade and Thompson [48] who showed that the enhancement was a function of the surface area of alumina particles. In the study of Shiuli and Shahi [49] the maximum enhancement recorded was about 2 orders at 302K for 10 m/o of Al_2O_3. The SEM showed that the distribution of Al_2O_3 was not uniform and the particles of Al_2O_3 of 0.05 μm agglomerated to 0.5 μm.

The occurrence of highly conducting phase found to be present in these systems was studied by Chen Liquan in LiCl;η-Al_2O_3 [46] with mole percent and temperature and Takeshi and Shichio [50] in LiBr-Al_2O_3 from Li NMR spin relaxation times. The amount of this highly conducting phase was found to increase with the amount of dispersed oxide at lower m/o Al_2O_3 and was found to be constant later up to 50 m/o, which means that the thickness of highly conducting phase layer was maintained constant up to 50 m/o of Al_2O_3. This layer was found to decrease linearly with Al_2O_3 content beyond 50 m/o. This explains the composition dependence of enhancement effect.

II.2 FLUORITES

The enhancement of conductivity in fluorides of Ca and Ba was observed by Fujitsu et al. [51] by dispersing with Al_2O_3 particles of sizes 0.3 and 0.06μm. In CaF_2-Al_2O_3 system a maximum enhancement of 1-2 orders of magnitude was observed for 0.06μm at 5 m/o of Al_2O_3 and for 0.3μm at 10m/o of Al_2O_3 at 500°C and it was found to depend on composition as well as particle size of Al_2O_3. A similar variation could be observed in BaF_2 - Al_2O_3 where maximum was observed for 20m/o Al_2O_3 at 500°C for 0.3 and 8μm particles. Explanation for the composition and particle size dependence of conductivity assumed the formation of highly conductive interface between host matrix and Al_2O_3 particles. The conductivity and the thickness of the interface layer at 500^oC were estimated to be 10^{-3} S/cm and 0.3 to 0.6μm respectively by simple mixing model. Addition of Al_2O_3 or ZrO_2 to the polycrystalline CaF_2 [52] was found to increase the conductivity relative to host material. The maximum enhancement was recorded to be 2 orders of magnitude for 10m/o Al_2O_3 powder of the higher surface area from Alcoa Co. and for 5m/o Al_2O_3 samples of lower surface area from Adolf Meller Co. in the low temperature region as well as a decrease in the activation energy for conduction compared to pure CaF_2. The 25m/o composites of both types of alumina showed a decrease in conductivity which was attributed to blocking effects of the insulating Al_2O_3 phase created in the composite.

In ZrO_2 dispersed system a more systematic conductivity behavior was observed where the maximum enhancement occurs at 5m/o in both high and low temperature regions. Increased concentration of fluorine ion interstitials at the interface was thought to be responsible for such enhancement [53]. Measured transport number of fluorine ions in these composites was in support of the above conclusion. The increase in the conductivity was studied in Al_2O_3, CeO_2 dispersed CaF_2 systems by vaidehi et al., [54]. The maximum enhancement observed in Al_2O_3 dispersed system was 2 orders, whereas in CeO_2 dispersed system it was about 3 orders of magnitude at 650^o K with respect to pure CaF_2. Build up of space charge regions at the phase boundaries of dispersed solid electrolyte systems were postulated to cause the enhancement of their ionic conductivities. Some aspects of the increase in the ionic conductivities of this system were explained by Maier's semi-quantitative model based on quasi-parallel switching. It was proposed that a substantial enhancement in the vacancy concentration of CaF_2 brought about by the attraction of F^- ions to the surface of Al_2O_3 (or CeO_2) was responsible for the low temperature increase in the conductivity of CaF_2.

The enhancement recorded in fluorite type material $SrCl_2$-Al_2O_3 system [55] was observed to depend on the composition and the grain size of Al_2O_3 and the method of preparation. The particle sizes used in this study were 0.06, 0.3, 1, 3, 8 and 15µm. These Particle sizes were found to aggregate into larger secondary particles during the sample preparation and their average particle sizes were measured to be 2.6, 8.2 and 10µm whose original sizes were 0.3, 3 and 8µm respectively. It was considered that the interface between $SrCl_2$ matrix and Al_2O_3 particles played a major role in giving rise to high ionic conductivity. The conductivity enhancement was estimated to be 2 orders of magnitude while the thickness of the interface layer was estimated by simple mixing model to decrease with increase in temperature from 0.6 to 0.15µm.

In order to evaluate the validity of the estimations made by simple mixing model the conductivity studies on a multi-layered sample were undertaken by the authors (Fujitsu et al.) [55]. This multi-layered sample was prepared by dispersing $SrCl_2$ in sec-butyl alcohol and using this solution to paint both the surfaces of Al_2O_3 as thin plates (50µm.), which were laminated upon each other and finally sandwiched between two thick Al_2O_3 plates. The current was measured parallel to the interface layers. It was observed that the calculated conductivity was slightly higher than the measured conductivity and this was attributed to the imperfect contact between Al_2O_3 plates and $SrCl_2$ layers or due to an experimental error. This experiment leads the authors to believe in the formation of an interfacial layer of sub micron size between the $SrCl_2$ and Al_2O_3 that produced the enhancement effects.

Two probe ac impedance measurements carried out on PbF_2 when dispersed with CeO_2, SiO_2, ZrO_2 and Al_2O_3 in the frequency range 10 HZ to 10^5 HZ showed an enhancement in the extrinsic conduction [56] region. The adsorption of water was estimated to be 0.1% and 0.2% in Al_2O_3 and SiO_2 respectively when they were exposed to air at room temperature. No new phase was detected by X-Ray powder diffraction in any of the mixtures. The conduction mechanism was explained on the basis of the space charge layer formed at the oxide/host interface which was determined by the chemical reactions at the interface. These interactions were discussed by comparing with particle hydrates. A particle hydrate is a composite consisting of colloidal sized particles dispersed in an immobilized aqueous solution. Proton conduction occurs in this immobilized aqueous matrix. If aqueous matrix is initially pure water, then the analogy with a colloidal particle dispersed in a stoichiometric salt is nearly exact except for the crystalline character of the salt.

II.3 ALKALINE EARTH NITRATES

Enhancement of dc ionic conductivity is in dispersed solid electrolyte system $Sr(NO_3)_2$-Al_2O_3 was studied by Narender Reddy et al [57-58]. The maximum enhancement of about 3 orders is observed for 29.3m/o of $Sr(NO_3)_2$-Al_2O_3 system. XRD showed no evidence of formation of any solid solution and as per them the very high melting point of the insulator Al_2O_3 also could be a reason why it cannot form a solid solution. Enhancement of conductivity was explained on the basis of the formation of space charge layer. $Sr(NO_3)_2$, being a anti-frenkel type defect solid, enhancement observed in it could be understood as follows: The interaction between the mobile ions of MX and the dispersoid D leads to the formation of vacancies of mobile ion species in the space charge region near the MX/D interface. This can happen both when the mobile ions are attracted to the phase D leaving the vacancies at the interface and repelled in to the matrix MX to form interstitials. Of these the formation of vacancies was thought to be more probable then the formation of interstitials.

They extended their studies on the role of particle size (36.9, 0.3 and 0.06μm) and mole percent of the dispersoid in $Sr(NO_3)_2$:Al_2O_3 [59] composite solid electrolyte system. The enhancement of conductivity was observed to depend on the size of the particle, however, for a given specific surface area it was found to be same for all the three particle sizes. Enhancement of conductivity was noticed to increase with mole percent of the dispersoid in the extrinsic temperature region. The decrease of enhancement at higher mole percent was attributed to the clustering of dispersoid particles due to the decrease in the total surface area available to interact with the host material.

III THEORETICAL MODELS

Several phenomenological theories have been proposed to understand the ion transport mechanism in composite electrolyte systems. No single unified model exists, as yet, which can explain uniquely various experimental results on different composite electrolyte systems. However, the central feature of the majority of the models, suggested to explain conductivity enhancement in two-phase composite systems, is the existence of a space-charge region (called double layer) at the interface between the host and dispersoid. Various experimental studies have been directed towards this theme, namely dependence of conductivity on the surface area [60, 61] of alumina, apparent effect of surface hydration [61], etc.

In addition to this, bulk interactions have also been suggested as a cause for conductivity enhancements in some composite systems [62]. Most of these models focus on the calculation of compositional dependence of conductivity. They differ only in the methods of calculation and in the assumptions concerning the distribution of the dispersoid particles in the composite system. Some important models proposed for composite electrolyte systems are discussed below.

III.1 JOW AND WAGNER'S MODEL

Kliewer [63] proposed the continuum model for the space charge region near surfaces of Frenkel disorder type compounds(like CuCl) to describe the case of space charge regions surrounding spherical inclusions in matrix material of Frenkel type. In order to explain conductivity enhancement in a CuCl-Al_2O_3 composite electrolyte system, Jow and Wagner [61] extended Kliewer's theory. They assumed that a space charge region is created at the host and dispersoid interface boundary when a dispersoid phase (A) is introduced in to the electrolyte host matrix (MX). A space charge layer of thickness λ has been created around the dispersoid particles. Figure III.1 shows the idealized spherical particle and cross-sectional view for analytical calculation. They proposed that the dispersoid particle has a charge, though the spin is not known, at near the surface, which is compensated by the formation of oppositely charged defects in the diffused space charge. As a result, an excess defect concentration in this region is formed.

Jow and Wagner attributed this unexpected enhancement to the space charge region formed near the interface between the matrix electrolyte and the inert second phase. The result of the deduced conductivity for the low content of the second phase was shown as

$$\sigma = \sigma_0 + 3e\mu <\Delta n> \lambda (1/r)(P /1-P) \qquad (1)$$

Where σ is the ionic conductivity of the matrix material in the bulk, e is the absolute electronic charge, $<\Delta n>$ the average excess charge density in the space charge

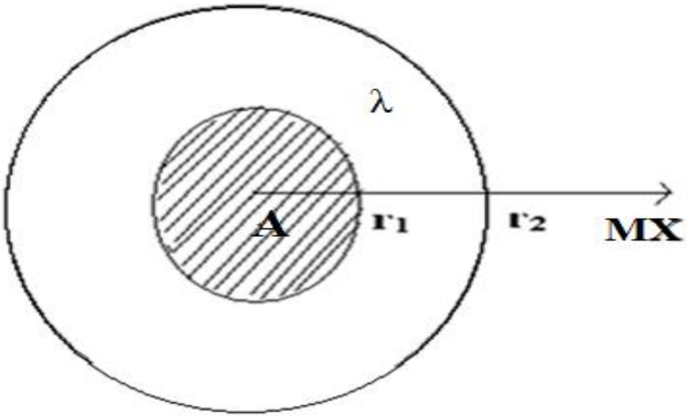

Fig. III.1 Schematic cross-sectional view of single alumina particle in a host matrix.

region, μ the mobility of the ion or defect species in the matrix material, λ the Debye length, r the radius of the dispersoid of the second phase and p the volume content of the second phase. This model agreed well with the experimental results at low concentrations of the second phase. With regard to the limit of the assumption that the second phase should be much smaller than that of the matrix. This model therefore cannot account for maxima of conductivity observed in several cases for a given mole percentage of the dispersoid.

III.2 MAIER'S MODEL

Maier [64-66] has proposed, an approach for estimating the bulk ionic conductivity in an ionically conducting matrix MX dispersed with insulating second phase A. In this it is considered that there is no solubility or chemical reaction except that there is a possibility of surface interaction which is known to occur with oxides between the host matrix MX and insulating phase A. He has also discussed the defect chemistry involved in the space charge region at the interface which is responsible for the conductivity enhancement. The surface interactions at the interface results in the formation of space charge which is exponentially decreases with x (distance) into the interior. The defect reaction at the interface is understood by splitting it into the formation of the bulk vacancies and interstitials in Frenkel type solid.

$$M_M + V_A \leftrightarrow M'_A + V^1_M \qquad (2)$$

$$M'_A + V_1 \leftrightarrow M'_1 + V_A \qquad (3)$$

The first part of the reaction is that when a cation in normal lattice (M_M) goes on to the interface (assuming that there is a vacancy at interface site V_A) and becomes an interfacial cation (M'_A) creating a vacancy in its normal lattice position (V^1_M). In the second part, interface cation (M'_A) will be moved to interstitial position (assuming that there is an interstitial vacancy at V_1), and becomes interstitial cation (M'_1), leaving the interface site vacant again. $\Delta_{VA}G^0$, $\Delta_{IA}G^0$ are the free energies required for the formation of vacancy and interstitial respectively in the presence of the second phase and $\Delta_{S1}G^0$ is the energy required for the surface interaction due to the presence of the second phase A. The corresponding interaction is given by

$$M_S + V_A \leftrightarrow M'_A + V_S \qquad (4)$$

Where M_S is a surface cation. In this, two cases are possible. One is stabilization of M surface ion by the second phase i.e., an attractive interaction between MX and A-phase. A possible mechanism is shown in Figure III.2(a). If the energy of this mechanism is sufficient enough to compensate the entropic effects, the free energy of the vacancy formation is lowered and that of interstitials is increased compared to the intrinsic values. If $\Delta_{VA}G^0 < \Delta_{IA}G^0$, the surface interaction has the consequence that ions will be sucked out of the volume and the concentration of vacancies will be increased. On the other hand, the M ions will be pushed into interstitial sites (repulsive interaction between A and M_s) as in Figure III.2(b). Therefore, in both the cases for sufficiently strong interactions, an extrinsic conductivity enhancement is to be expected. This model treats the space-charge region as separate phase and considers each phase as a parallel resistor. The total conductivity is given by

$$\sigma = \beta_A \varphi_A \sigma_A + \beta_\alpha \varphi_\alpha \sigma_\alpha + \beta_{SC} \varphi_{SC} \sigma_{SC} \qquad (5)$$

Where α denotes the bulk, A denotes the insulating phase and SC space-charge region. φ_A is the volume fraction of the phase A, β is a parameter describing the deviation from the ideal parallel switching. The physical situation is shown in figures III.3 (a) and (b).

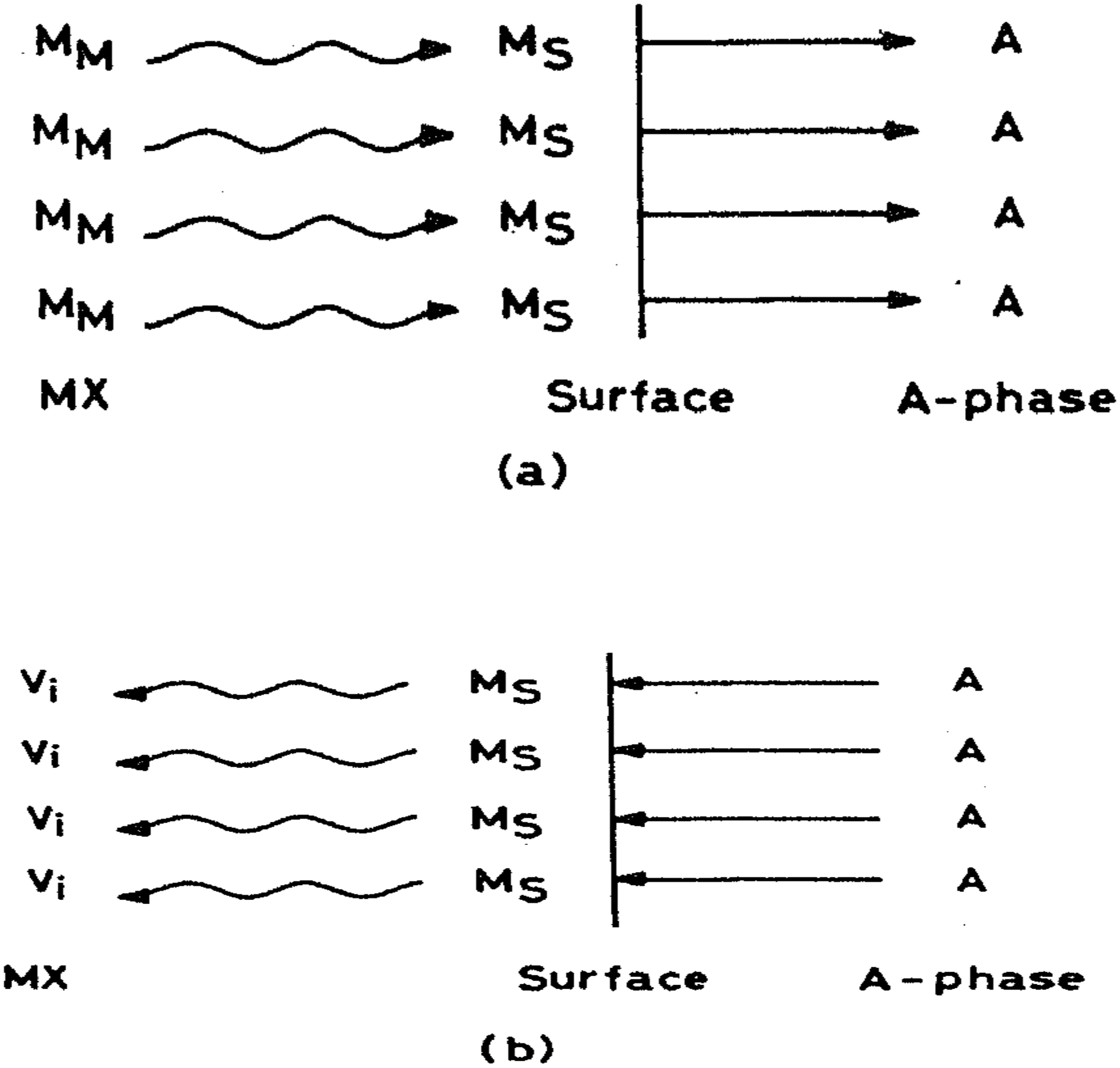

Fig. III.2 The surface effects of a phase on host matrix

(a) An attractive interaction results in enrichment of vacancies.

(b) A repulsive interaction in driving M_S surface ions into interstitial positions.

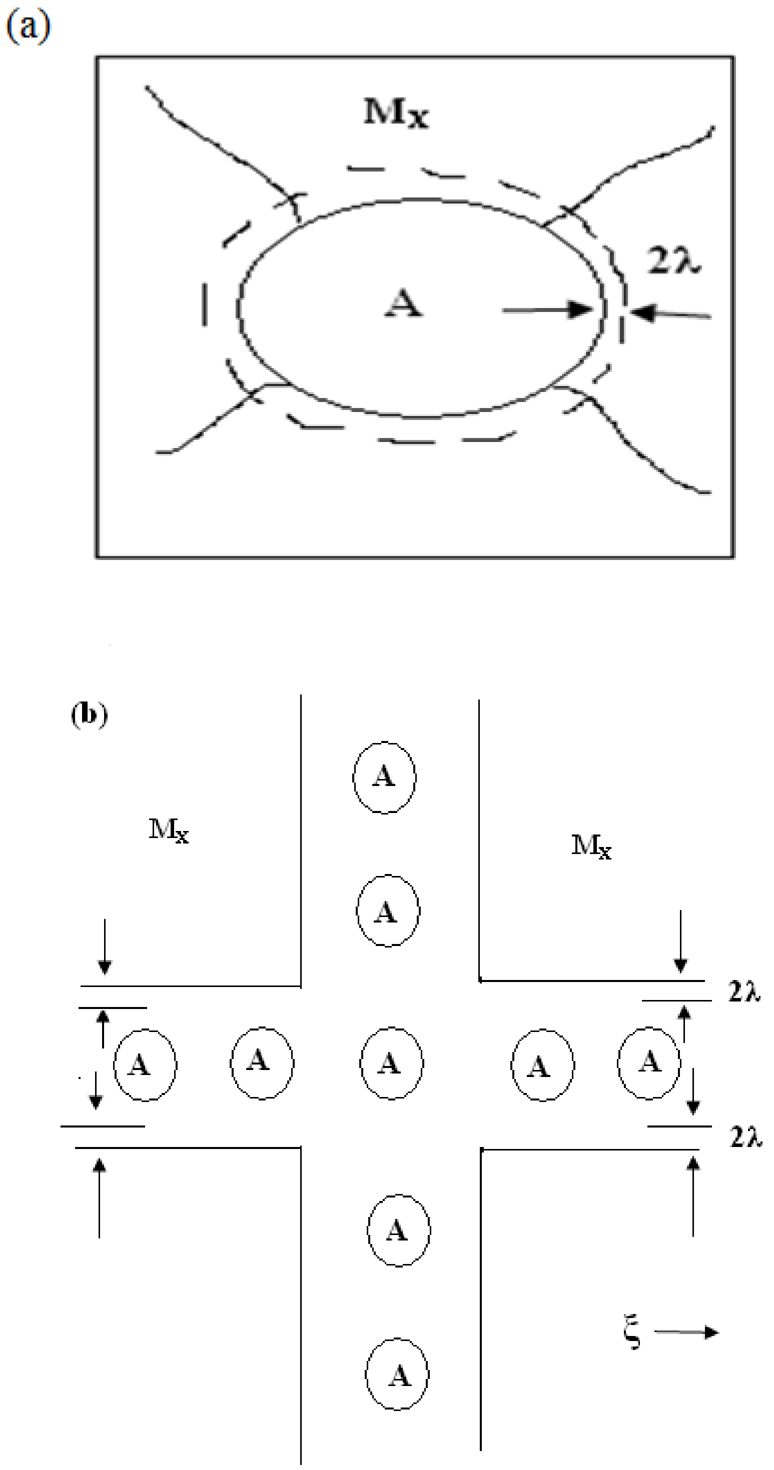

Fig III.3 (a) Phase A particle embedded in MX material and bearing a space charge layer

(b) Coherent Phase A spheres forming crossing chains or areas.

The conductivity component due to the space charge region, from eq.(1) may be written as

$$\sigma_{SC} = e\,(2\lambda)\,\mu_V\,(C_{V0}\,C_{V\alpha})^{1/2} \qquad (6)$$

here μ_V is the mobility of vacancies. C_{V0} and $C_{V\alpha}$ are the concentrations of vacancies at the surface and the bulk respectively. 2λ is the effective thickness of the space charge layer. The dispersoid particles are assumed to be spherical and surrounded by a space charge region of thickness 2λ. The volume fraction of the space charge layer is obtained by subtracting the volume fraction of inner sphere from that of the outer sphere and is given by

$$\varphi_{SC} = 3\,(2\lambda / r_A)\,\varphi_A \qquad (7)$$

where r_A is radius of the dispersoid particles, so the total conductivity from eqn. (6) is given by

$$\sigma = (1-\varphi_A)\,\sigma_\alpha + 3e^{\beta}{}_{SC}\,2\lambda\,(\varphi_A / r_A)\,\mu_V\,(C_{V0}\,C_{V\alpha})^{1/2} \qquad (8)$$

By adjusting the ideal parallel switching parameter, ${}^{\beta}{}_{SC}$, in the range 0.2-0.7 depending upon distribution topology, it has been seen that the above equation explained experimental results such as larger conductivity enhancement at low temperatures, particle size dependence, effect of wet dispersoid etc., for various solid electrolyte systems fairly well. The attractive feature of Maier's model is that it highlights the mechanism responsible for enrichment of surface defects in the space charge region. Although, Maier's model explains many characteristic features of composite electrolyte systems well, it failed on several points such as: Maxima in σ versus φ_A plots, the assumption of an oversimplified distribution topology being characterized by a β –factor and resulting in quasi-parallel switching, the assumption of spatially constant values for mobility, the dielectric constant and the molar volume, neglecting the structural changes, polarization effect , elastic effects etc.

REFERENCES

1) R.W.G. Wyckoff, ‘Crystal structures’, Interscience pblishers, 2,**(1964)**, 480.

2) R.W.G. Wyckoff, ‘Crystal Structures’ InterScience Publishers,1,**(1963)**,239.

3) L.Vegard, Z. Phys., 395,**(1922),** 410.

4) R. Birnstock, Z. Krist., 124, **(1967),** 310.

5) A.M. Bon, C. Benoit and O. Bernard, Phys. Stat. Sol.(b), 78, **(1976),**67.

6) R.Srinivasan, Proc. Indian Acad.Sci., 41A, **(1955)**, 49.

7) Sawada, S., Nomura, S. & Fujii, S. (1958). J. Phys. Soc. Jpn, 13, 1549.

8) M K Aydinol, JVMantese and S P Alpay, J. Phys. Condens. Matter, 19, **(2007)**, 210-23.

9) V.M. Patrov, N.I. Giricheva, V.N Petrova and G.V. Girichev Journal of structural chemistry,4,**(1991)**, 494-498.

10) Sawada, S., Nomura, S., Fujii, S., *J. Phys.Soc. Japan*, 13, **(1958),**1549.

11) Sawada, S., Nomura, S., Asao, Y., *J. Phys.Soc. Japan*, 16, **(1961),** 2486.

12) Nolta, J.P., Schubring, N.W., *Phys. Rev.Lett.*, 9, **(1962)**, 285.

13) Nolta, J.P., Schubring, N.W., Dork, R. A., *J.Chem. Phys.*, 42, **(1965)**, 508.

14) M K Aydinol, JVMantese and S P Alpay,. Journal of physics: Condensed matter 19, **(2007),** 496210, (23pp).

15) Neeraj Kumar, , Rabinder Nath, *J. Mater. Environ. Sci.* 2(4), **(2011),** 379-386 ISSN: 2528-2028.

16) H.G. MCADIE, Thermal Analysis (Proc. Of the 3rd ICTA, Davos, 1971), Birkhauser, Basel, 1, **(1972),** 591.

17) A.S. Lidiard, Hdb.Phys.Springer-Verlag, 20, **(1957)**.

18) J.Rolfe, Can.J.Phys.48, **(1964)**,2195.

19) M.M. Nekrasov, B.M. Belyakov and M.K. Rodionov, IZV.VUZ.FIZ (USSR) 4, **(1967),**11.

20) N. Nadler and Rossel, Phys. Stat. Solidi (a), 18, **(1973),** 711.

21) W. Lehfeldt, Z. Physik 85, **(1933),**717.

22) T.E. Phipps and E.G. Patridge, J. Am. Chem. Soc. 51, **(1929),** 1331.

23) H. Kelting and H. Witt, Z. Physik 26, **(1949),**197.

24) J.E. Ambrose and W.E. Wallace, J. Phys. Chem. 63, **(1959),**1536.

25) H. Schultze, Thesis university of Gottingen **(1952)**.

26) Yu. M. Annenkov and V. A. Grishukov, IZV. VUZ. FIZ (USSR), 74, **(1967),**11.

27) J. Arends, H.W. Den Hartog and A.J. Dekker, Phys. Stat. Solidi 10, **(1965),**105.

28) E. K. Zavadowskaya, J.S. Ivankina and I. Ya. Melik Gaikazyan, IZV. VYW. UCHAB, ZAB. FIZ, 12, **(1970),**92.

29) U.V.Subbarao and V.Haribabu, Crystal Lattice defects, 8, **(1978),** 21-26.

30) P. Veeresham, Dr. U. V. Subba Rao, Dr. V. Hari Babu, 18,12, **(1983),**1581-1584.

31) K. Shahi, J.B. Wagner Jr., Journal of physics and chemistry of solids, 43, 8 , **(1982),**713-722.

32) S.L. Garud and K.B. Saraf, Bull Mater. Sci, 31, 4, **(2008),**639-643.

33) C.M. Padma, C.K. Mahadevan, Materials and Manufacturing Processes, 23, 2, **(2008),** 143-150.

34) Jayaram, " Optics and spectroscopy part 1 Tm," Tn Tbs, New Delhi, **(1972)**.

35) J. Kudnovsky, N.E. Christensen, J. Masek, Physical Review B, 43, **(1991),** 15.

36) Wen-Ming Chien, Dhanesh Chandra, Jennifer Franklin, Claudia J. Rawn and Abdel K. Helmy, JCPDS, 48, **(2005)**.

37) Jander, W., Z.Angew. Chem., 42,**(1929)**,462.

38) Wanger,C., J.Phys.Chem.Solids, 33, **(1972)**,1051.

39) Crosbie, G., J Solid state Chem., 25,**(1978)**,367

40) Liang, C.C., J.Electrochem.Soc., 120,**(1973),**1289.

41) Liang, C.C., and Bernette, L.M., J.Electrochem.Soc., 123 no.4, **(1976)**,453-458.

42) S.Pack, Abstract No.133, Electrochemical Society meeting, Los Angels,**(1979)**.

43) Takeshi Asai, Ching-Hsing Hu and Shichio Kawai, mat. Res.Bull.,22,**(1987)**,269-274.

44) Takeshi Asai, Ching-Hsing Hu and Shichio Kawai, Solid State Ionics, 26,**(1988)**,1-4.

45) Takeshi Asai, and Shichio Kawai, Solid State Ionics, 34,**(1989)**, 195-199.

46) Liquan Chen, Zonguan Zhao, Chaoying Wang and Lizirong Kexue Tongbo, 26,**(1981)**,308.

47) Nakamura,O.and Goodenough,J.B., Solid State Ionics, 7,**(1982)**,125-128.

48) Slade,C.T. and Thompson, M.,Solid State Ionics, 26,**(1988)**,287-294.

49) Shiuli Gupta, patnaik, S., Chaklanobis, S. Chaklanobis, S. and Shahi,K., Solid state Ionics,31,**(1988)**,5-8.

50) Takeshi Asai and Shichio Kawai, Solid State Ionics, 20,**(1986)**,225-229.

51) Fujitsu,S., Miyayama,M., Koumoto,K. and Yanagida,H., J.Mat.Sci., 20,**(1985)**,2103-2109.

52) Kandkar,A., Tare,V.B. and Wagner,J.B., Revue de Chemie Minerale, t.23,**(1986)**,274.

53) Wen,T.L., Huggins,R.A., Rabenau,A. and Weppner, W., Revue de Chimie Minerale, 20,**(1983)**,643.

54) Vaideshi,N., Akila, R., Shukla,A.K. and Jacob,K.T., Mat.Res.Bull., 21,**(1986)**,909.

55) Fujitsu,S., Koumoto,K. and Yanagida,H., SolidState Ionics, 18 and 19,**(1986)**,1146-1149.

56) Shukla,A.K., ManoharanR. And Goodenough,J.B., SolidState Ionics,26,**(1988)**,5-10.

57) S.Narender Reddy, A.Sadananda Chary and T.Chiranjivi, Solid State Ionics 34,**(1989)**,73-77.

58) S.N.Reddy, and A.S.Chary and T.Chiranjivi, J. of Materials sci-Mat. In Electronois.

59) S.Narender Reddy, A.S.Chary and T.Chiranjivi, Solid State Ionics, 66,**(1993)**,131.

60) shahi,k. and wagner, J.B., J.Solid State Chem.41,**(1982)**,107.

61) Jow and Wagner, J.B., J.Electrochem.Soc. 126,**(1979)**,163.

62) Chowdary,P., Tare,V.B. and Wagner J.B., J.Electrochem.Soc.,**(1985)**,123-124.

63) K.L.Kliewer, J.Phys.Chem.Solids, 27,**(1966)**,705.

64) Maier,J., Phys.Stat.Sol(b), 123,**(1984),**K89.

65) Maier,J., J.Mat.Res.Bull., 20,**(1985)**,383-392.

66) Maier,J., Prog.Solid.State Chem., 23,**(1995)**.